

A NEW TYPE OF ELECTROMAGNETICALLY PROPELLED VIBRATION ACTUATOR FOR APPEARANCE INSPECTION OF IRON STRUCTURE

*Hiroyuki Yaguchi¹

¹Faculty of Engineering, Tohoku Gakuin University, Japan

*Corresponding Author, Received: 21 Nov. 2020, Revised: 03 Dec. 2020, Accepted: 17 Dec. 2020

ABSTRACT: Due to economic development, many social infrastructures such as various large structures are being constructed around the world. Inspection and maintenance of social infrastructure such as huge bridges and tanks is one of the most important items in the world. In the present study, a new vibration actuator that extends the principle of operation invented by the authors was proposed and tested. New principle of operation for the actuator capable of reciprocating movement by controlling the phase of two vibration components has been considered. The principle of operation for the actuator was established by a very simple analysis. The experimental results indicate that reciprocating motion can be realized by controlling the phase of the vibration of the two vibration components. Experimental results reveal that this vibration actuator is able to pull a load mass of 190 g and the maximum efficiency of the actuator was about 12.5 % for the case with own-weight. The actuator was confirmed to be able to easily control the direction of movement with two-channel function generator and power amplifier.

Keywords: Vibration, Actuator, Phase difference, Electromagnetic force, Inertia force.

1. INTRODUCTION

Due to economic development, many social infrastructures such as various large structures are being constructed around the world. Inspection and maintenance of social infrastructure such as huge bridges and tanks is one of the most important items in the world. However, inspection of huge structures is very difficult due to site conditions. For this reason, various inspection robots have been developed to ensure worker safety and reduce costs.

Robots with various movement principles have been proposed for inspection of structures. As a typical type, the robot using a suction cup [1-3] or an elastomer [4] can move without selecting the material of the wall surface. However, in this type, when dust or dirt adheres to the wall surface, the attractive force is significantly reduced. A claw gripper robot [5, 6] has been proposed for movement on a concrete wall. The application of this robot was limited to concrete with rough surface. Flight robots such as propeller type [7] and drone [8, 9] are proposed. These require skill to operate and are easily affected by weather such as rain and wind. In general, because mobile robots independent of structure material require complex controls and many additional devices, the range of application is quite limited.

On the other hand, many robots have been proposed for movement on iron structures. There are a magnetic caterpillar type [10] and a wheel type [11, 12] as typical robots. In general, these robots capable of a magnetic substance wall climbing move at low speeds because of problems with controllability and high weight using the use of many electromagnetic motors and reducers. Therefore, a lightweight robot with excellent operability is required.

The authors invented a lightweight actuator with excellent operability and a very simple structure [13]. Furthermore, when this actuator is built into a robot, direct drive is possible without reduction gear mechanisms because this actuator has high propulsion force. However, the movement direction of this actuator was limited to one way direction.

In the present study, a new vibration actuator that extends the principle of operation invented [13] by the authors was proposed. New principle of operation for the actuator capable of reciprocating movement by controlling the phase of two vibration components has been considered. The principle of operation for the actuator was established by a very simple analysis.

In actual machine test to prove the principle of operation, the vibration actuator in which two

vibration components of the same specification are arranged orthogonally was prototyped.

The experimental results demonstrate that the maximum propulsion force of this actuator was 1.9 N and the maximum efficiency was about 12.5 %. In addition, the vibration actuator was confirmed to be able to easily control the direction of movement with two-channel function generator and power amplifier. The actuator was confirmed to be able to move on magnetic substances, such as iron rails.

In the future, this actuator will be equipped with a micro CCD camera for visual inspection of the iron bridge. Furthermore, the actuator is applicable to the inspection of the iron structures such as oil and gas tanks and power generation equipment.

2. STRUCTURE OF THE VIBRATION ACTUATOR OPERATING BY INERTIA FORCE

Fig. 1 shows a vibration actuator capable of movement on a magnetic substance proposed by

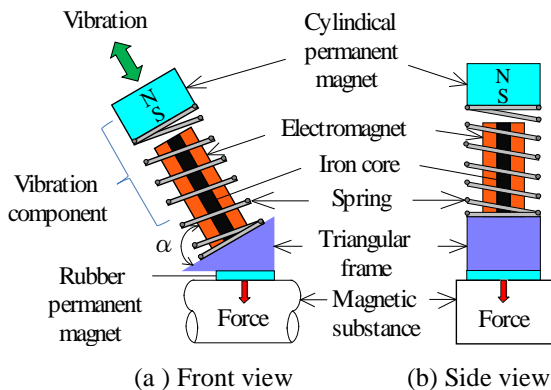


Fig. 1. Structure of the vibration actuator.

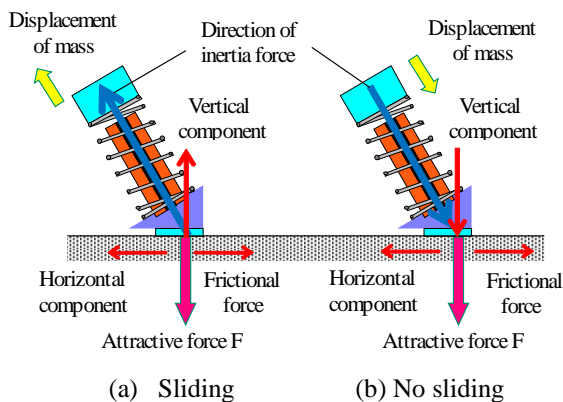


Fig. 2. Principle of locomotion.

the authors [13]. This vibration actuator is composed of a permanent magnet, a coil spring, an electromagnet, a triangular acrylic frame, and a rubber permanent magnet. When the diagonally mounted vibration component is excited by the electromagnet, an inertial force is generated in the diagonal direction. The angle α of the vibration component was set to 60 degrees based on the results obtained in a previous study [13]. The attractive force F generated by the rubber magnet attached at the support part acts on the vibration actuator when it is placed on a magnetic substance, as shown in Fig. 2. Therefore, the vibration actuator can vibrate on the magnetic substance.

The displacement coordinates x of the vibration component is determined in Fig. 2. As shown in Fig. 2(a), when mass m was displaced in the x direction, due to the vertical component of the generated inertial force, the attractive force F decreases and the frictional force decreases. When the horizontal component of inertial force exceeds the frictional force, the actuator can slide in the direction in which the vibration component is tilted. On the other hand, as shown in Fig. 2(b), when mass m was displaced in the $-x$ direction, the vertical component of the generated inertial force is superimposed on the attractive force F , and the frictional force increases. Therefore, the actuator cannot slide backward.

Because the horizontal component of the inertial force exceeds the frictional force, the vibration actuator is propelled by the difference between the frictional forces in the forward and backward directions acting on the rubber magnet in the support, as shown previous study [15]. This vibration actuator has a very simple structure and can generate propulsion about 10 times its own weight. However, the movement direction is limited to only one direction movement from the principle of operation.

3. STRUCTURE OF NEW VIBRATION ACTUATOR CAPABLE OF RECIPROCATING MOVEMENT

Fig. 3 shows a new vibration actuator capable of reciprocating movement. This vibration actuator is composed of two vibration components A and B having the same specifications, an acrylic frame and plate, and two rubber permanent magnets. Vibration components A and B are orthogonally arranged on an acrylic frame. The vibration

component is composed of a coil spring, a ring-type permanent magnet, and an electromagnet having a bobbin-type iron core proposed in the previous paper [14].

Magnetic field generated by electromagnet can be converted to electromagnetic force with high efficiency. Details of the vibration component and the bobbin-type iron core are shown in Fig. 4. The coil spring is a compression coil spring with a free length of 25 mm, an outer diameter of 12 mm, and a spring constant $k = 2689 \text{ N / m}$. The ring-type permanent magnet is NdFeB magnet with an outer diameter of 12 mm, an inner diameter of 9 mm, a thickness of 8 mm and magnetized in the height direction. For the electromagnet, the experimental results of the optimization of the bobbin-type iron core shape and the number of turns performed in the previous results [14] were applied. As shown in Fig. 3, the diameter of an iron disk is $D = 8 \text{ mm}$, thickness is $h = 1 \text{ mm}$, and diameter of shaft is $d = 3 \text{ mm}$ and the length is $H = 26 \text{ mm}$. The electromagnet was produced by winding a copper wire having an outer diameter of 0.14 mm around a bobbin-type iron core 1200 turns. Details of the electromagnet are shown in Table 1.

The two vibration components are glued on the acrylic frame. Two rubber permanent magnets were attached to the bottom of the acrylic frame to hold the actuator on the magnetic substance. One is a main rubber permanent magnet for holding the actuator on a magnetic substance. Another sub-rubber permanent magnet was attached to achieve stable straight movement. This main rubber magnet has a length of 13 mm, a width of 15 mm, and a thickness of 3 mm. The average surface magnetic flux density measured using a tesla meter was 128 mT. The sub rubber magnet has a length of 6 mm, a width of 15 mm, and a thickness of 3 mm. The average surface magnetic flux density was 121 mT. When the vibration actuator is set on

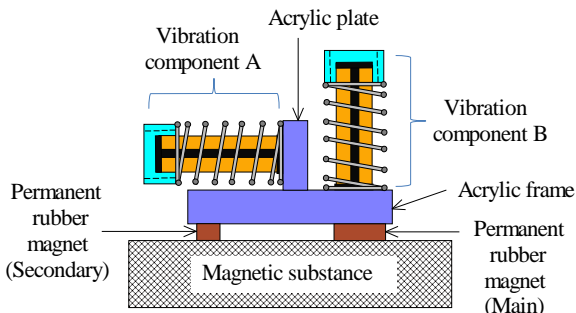


Fig. 3. Structure of the new vibration actuator. capable of reversible motion.

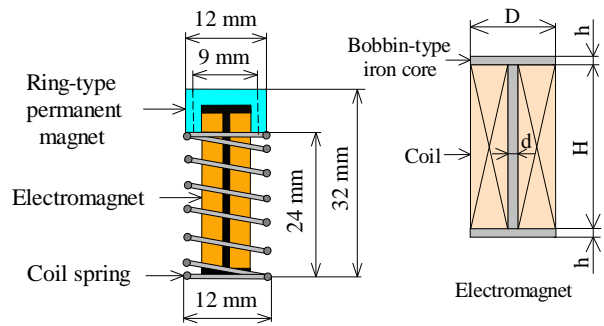


Fig. 4. Vibration components and electromagnets.

an iron structure, the attractive forces of the main and sub permanent magnets are $F_m = 5.2 \text{ N}$ and $F_s = 0.5 \text{ N}$, respectively. The vibration actuator has a height of 43 mm, a length of 58 mm, a width of 20 mm, and a total mass M_a of 39 g.

4. PRINCIPLE OF OPERATION FOR NEW VIBRATION ACTUATOR

As shown in Fig. 3, when two vibration components A and B are arranged orthogonally, the movement direction of the new vibration actuator can be changed by controlling the phase of the vibration in each component. The cases of

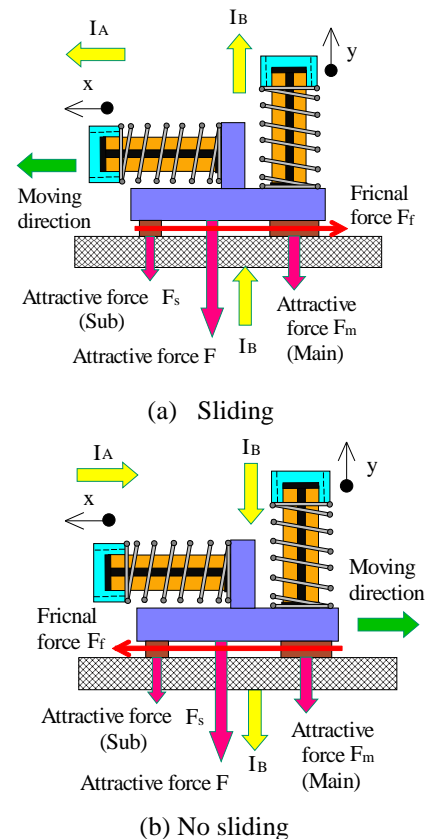


Fig. 5. Principle of reversible motion (In-phase).

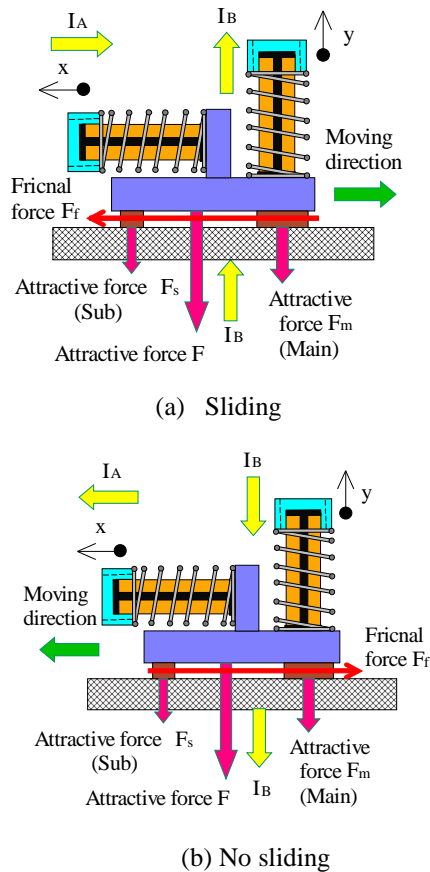


Fig. 6. Principle of reversible motion (Out-of-phase).

displacement in the horizontal and vertical directions are referred to as the vibration components A and B, respectively. The displacement coordinates x and y of each of the vibration components A and B are determined as shown in Fig. 5.

When the vibration actuator is set on a magnetic substance, the frame of this actuator is held by the main and sub rubber permanent magnets with the attractive force of F_m and F_s . Due to this reaction, the vibration component can be displaced. It was assumed that the vibration components A and B were vibrating at the angular frequency ω . The period of the vibration component in this case is τ , respectively.

First, as shown in the Fig. 5(a), consider a case where the phase difference between the vibration components A and B is 0 degree (in-phase). Focusing on one cycle ($\tau = 2\pi/\omega$) in the vibration component B, the holding force F and the frictional force F_f of the support part for the actuator change periodically as shown in Equation (1) due to the inertial force I_B by the permanent magnet of the vibration component B.

$$F = F_m + F_s - I_B \sin \omega \tau \quad (0 < \tau < \pi/\omega), \quad F_f = \mu F \quad (1)$$

where, t is time, and μ is the friction coefficient. When the component A is displaced in the $+x$ direction in the same phase while the vibration component B is displaced in the $+y$ direction, the vibration actuator easily slides in the $+x$ direction. As shown in equation (2), when the inertia force I_A of the permanent magnet in the vibration component A exceeds the friction force F_f , the actuator can move in the $+x$ direction.

$$I_A > F_f \quad (2)$$

On the other hand, as shown in Fig. 5(b), when the vibration component B is displaced in the $-y$ direction, the holding force F and the frictional force F_f increase as shown in Equation (3) due to the inertial force I_B by the permanent magnet.

$$F = F_m + F_s + I_B \sin \omega \tau \quad (\pi/\omega < \tau < 2\pi/\omega), \quad F_f = \mu F \quad (3)$$

Even if the component A is displaced in the $-y$ direction in opposite phase, the inertia force I_A cannot exceed the friction force F_f . Therefore, the actuator cannot move as shown in Equation (4).

$$I_A < F_f \quad (4)$$

The actuator can move in one direction by changing the frictional force of the rubber permanent magnet attached to the frame.

Fig. 6 shows a case where the phase difference between the vibration components A and B is 180 degrees (opposite phase). The actuator can move in the $-x$ direction according to the principle of movement by the frictional force and the inertial force described above. Accordingly, the present actuator can change the movement direction between forward and backward by controlling the phase of the two vibration components.

5. BASIC CHARACTERISTICS OF THE NEW VIBRATION ACTUATOR

The basic characteristics of the new vibration actuator capable of the reciprocating movement were investigated. Fig. 7 shows an outline of the experimental apparatus. In the experiment, two vibration components were driven resonantly by a two-channel signal generator and amplifier. The resonance frequency is 128 Hz. The voltage, current and power input to the electromagnet in the vibration component were measured by a power analyzer. As the magnetic substance, an iron rail having a width of 50 mm, a thickness of 50 mm, and a length of 500 mm was used. In the measurement, the vibration actuator was set on a

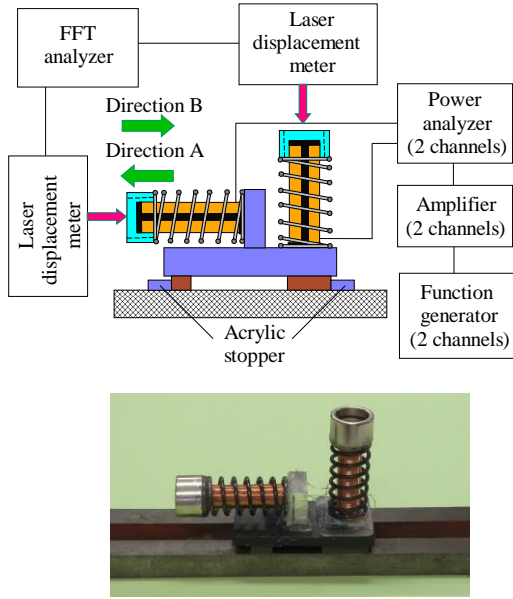


Fig. 7. Experimental apparatus and actuator.

horizontal plane. As mentioned above, the attractive forces by the main and sub rubber permanent magnets are $F_s = 5.2 \text{ N}$ and $F_m = 0.5 \text{ N}$. The coefficient of friction between the rubber permanent magnet and the iron rail is 0.84. The directions of movement of the actuator are respectively defined as shown in Fig. 7.

Fig. 8 shows the relationship between the input current to each electromagnet and the displacement amplitude in the vibration components A and B. Using an acrylic stopper, the state where the vibration actuator is freely held has been set. For the measurement of the displacement amplitude, a laser displacement meter and an FFT analyzer were used as shown in Fig. 7. As shown in the figure, in both vibration components, the displacement amplitude increases almost linearly with an increase in the input current. Therefore, the displacement amplitude in each vibration component can be estimated by measuring the input current.

The input current to the electromagnet of the vibration component B is set to 50 mA, and Fig. 9 shows the relationship between the vibration amplitude of the vibration component A and the speed of movement for the vibration actuator. In this case, the two acrylic stoppers were removed. As shown in Fig. 7, the Direction A (Forward) is a case where the phase difference of displacement between the vibration components is 0 degree, and the Direction B (Backward) is a case where these phase differences are 180 degrees. The speed

varies greatly depending on the movement direction. The average value of the movement speed in the Direction B is 0.68 times that in the Direction A. This is due to the attractive force of the sub rubber permanent magnet attached to the support part of the actuator. However, as described above, the movement speed of the actuator almost depends on the displacement amplitude. By controlling the input current to the electromagnet, the movement speed in both directions can be adjusted the same.

The input current to the electromagnet of the vibration component A at 50 mA was set, and Fig. 10 shows the relationship between the vibration amplitude of the vibration component B and the movement speed of the vibration actuator in two directions. As the input current to the vibration component B increases, the holding force of the actuator increases. Due to the increase in the holding force, the vibration amplitude of the two vibration components increases, so that the movement speed increases. For the reasons

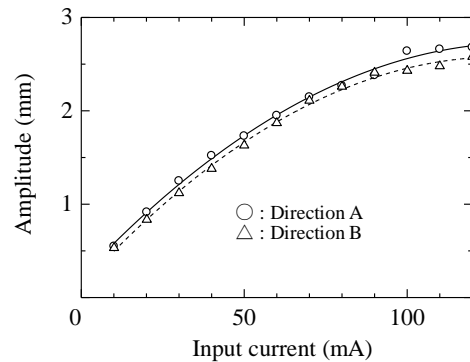


Fig. 8. Relationship between the input current and the amplitude.

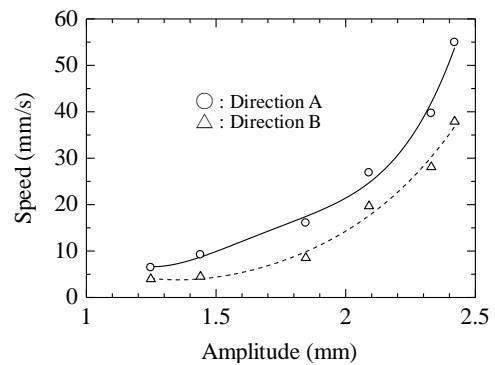


Fig. 9. Relationship between the amplitude and the speed (For fixed input power to component B).

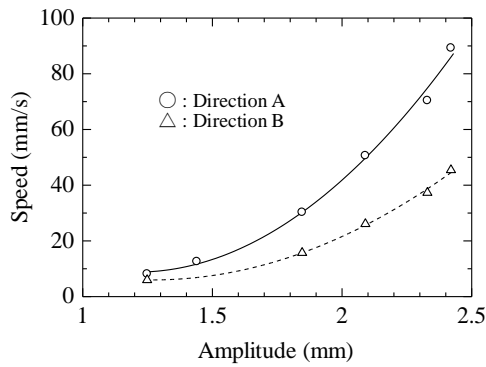


Fig. 10. Relationship between the amplitude and the speed (For fixed input power to component A).

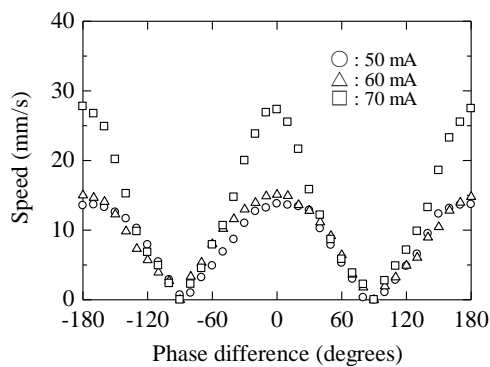


Fig. 11. Relationship between the phase difference and the speed.

described above, also in this result, a difference in speed occurs depending on the movement direction.

Fig. 11 shows the relationship between the phase difference in the vibration components A and B and the movement speed. The input current to the electromagnet in both vibration components was varied to 50, 60, 70 mA. In this case, the vibration components A and B were vibrated at 128 Hz, and the phase of the component A was changed from -180 degrees to 180 degrees using the phase adjustment of the two-channel signal generator. The movement speed shows the maximum value when the phase difference is 0 degree and 180 degrees. In these cases, the movement speed of the actuator is about 30 mm / s. When the phase difference is -90 degrees and 90 degrees, the vibration actuator cannot move due to the movement principle.

6. MOVEMENT CHARACTERISTICS OF THE VIBRATION ACTUATOR

As shown in Fig. 12, the tilt angle of the iron rail was set to β_1 and β_2 , and the movement

characteristics of the vibration actuator were measured. In the experiment, the phase difference in each vibration component was set to 0 degree and 180 degrees.

Figs 13 and 14 show the relationship between the tilt angle β_1 , β_2 of the iron rail and speed for the Direction A (Forward) and the Direction B (Backward) of the vibration actuator by changing the input current to the electromagnet in each vibration component. In the figure, -90 degrees indicates vertical downward movement, 0 degrees indicates horizontal movement, and 90 degrees

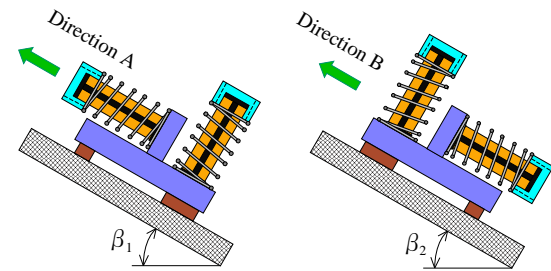


Fig. 12. Vibration actuator moving on the iron rail with tile angle.

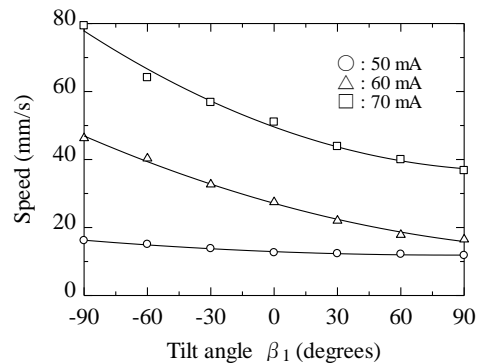


Fig. 13. Relationship between the tilt angle and the speed (In the case of β_1).

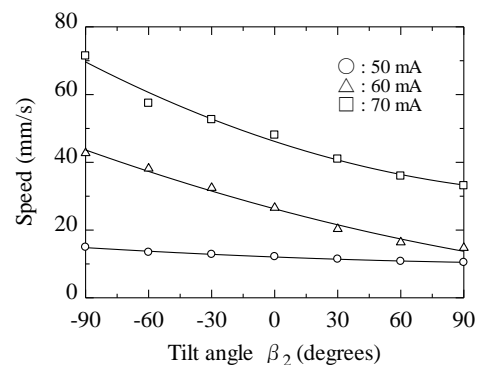


Fig. 14. Relationship between the tilt angle and the speed (In the case of β_2).

indicates vertical upward movement. As the tilt angle of the iron rail increases, the movement speed of the actuator decreases. This is due to the weight of the actuator itself. The actuator can move with almost the same tendency in the forward and backward directions.

The load mass was attached to the frame of the actuator using a string. The tilt angle of the iron rail was set to 90 degrees. Figs 15 and 16 show the relationship between the load mass mounted on the actuator and the vertical upward speed when the actuator moves forward and backward direction. The input current to the electromagnet in each vibration component was changed from 50 mA to 110 mA in three types. As shown in the figure, the maximum pulling force of the actuator in the case of forward movement is 1.9 N, while that in the case of backward movement is only 1.3 N. As described above, this is because the attractive force of the sub rubber permanent magnet has an effect. The presence of the attractive force asymmetric with respect to the vibration component B degrades the movement characteristics of the

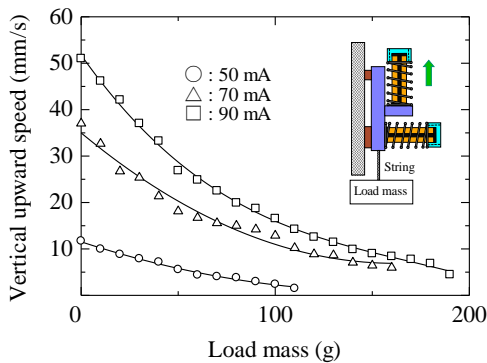


Fig. 15. Relationship between load mass and vertical upward speed (Direction A).

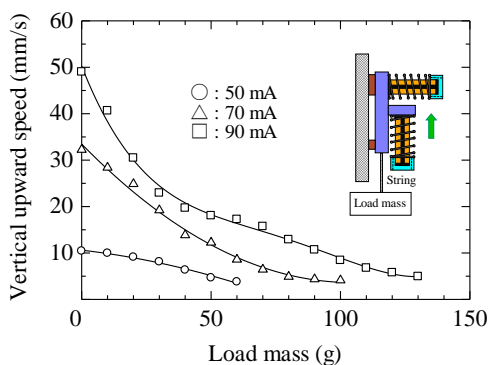


Fig. 16. Relationship between load mass and vertical upward speed (Direction B).

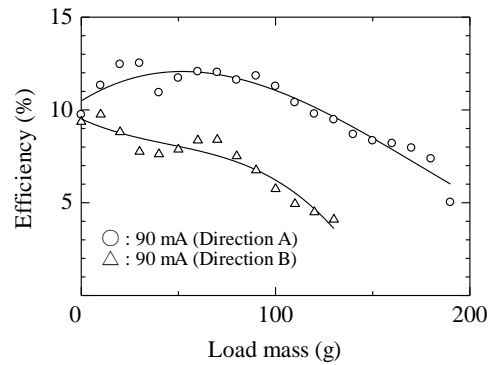


Fig. 17. Relationship between load mass and efficiency.

actuator. However, the sub rubber permanent magnet is needed to drive the actuator straight.

Fig. 17 shows the relationship between the load mass and the efficiency of the vibration actuator. The efficiency η is expressed as follows:

$$\eta [\%] = (M_a + M_m) v_{up} g \times 100 / P_i \quad (5)$$

where M_a is the total mass of the actuator, M_m is the load mass, v_{up} is the vertical upward speed, g is the acceleration due to gravity, and P_i is the input power. The solid line indicates the results of the Direction A (Forward) for the actuator pulling its own weight, and the dashed line indicates the results of the Direction B (Backward). The maximum efficiency of the actuator was about 12.5 % for the case of direction A.

7. CONCLUSION

A new type of a vibration actuator capable of reciprocating movement by means a phase difference between the two vibration components has been proposed and tested. It was proved by the actual machine that the movement direction can be switched by controlling the phase between the two vibration components with two-channel function generator and power amplifier. The principle of operation for the actuator was established by a very simple analysis and the actual machine.

Experimental results reveal that this vibration actuator is able to pull a load mass of 190 g. The maximum efficiency of the vibration actuator was about 12.5 % for the case with own-weight. However, because the attractive force at the frame of the actuator is asymmetric, there was a difference in the speed depending on the movement direction. It is necessary to improve the orthogonally arranged vibration components to a

symmetrical type.

In the future, the realization of the 3-axis orthogonal arrangement of vibration components enables the development of actuators for driving robots. Furthermore, it is necessary to increase the propulsion force by redesigning the magnetic circuit and vibration components.

8. ACKNOWLEDGMENTS

I would like to thank the students of Yaguchi Laboratory and the staff of the machine factory of Tohoku Gakuin University for their involvement in this research.

9. REFERENCES

- [1] Fukuda T, Matsuura H., Arai F., Nishibori K., Sakauchi H. and Yoshi N., "A Study on Wall Surface Mobile Robots", *Trans. Japan Soc. Mec. Eng.*, vol. 58, no. 550, 1992, pp. 286-293.
- [2] Subramanyam A., Mallikarjuna Y., Suneel S. and Bhargava L. K., "Design and Development of a Climbing Robot for Several Applications", *International Journal of Advanced Computer Technology*, Vol. 3, No. 3, 2011, pp. 15-23.
- [3] Wang W., Wang K., Zhang H. and Zhang J., "Internal Force Compensating Method for Wall-Climbing Caterpillar Robot", in *Proc., IEEE International Conference on Robotics and Automation*, 2010, pp. 2816-2820.
- [4] Kute M. Murphy Y. and Sitti M., "Adhesion Recovery and Passive Peeling in a Wall Climbing Robot using Adhesives", in *Proc., IEEE International Conference on Robotics and Automation*, 2020, pp. 2797-2802.
- [5] Xu F., Wang X., and Jiang G., "Design and Analysis of a Wall-Climbing Robot Based on a Mechanism Utilizing Hook-Like Claws", *International Journal of Advanced Robotic Systems*, Vol. 9, No. 261, 2012, pp.1-12.
- [6] Funatsu M., Kawasaki Y., Kawasaki S. and Kikuchi K., "Development of cm-scale Wall Climbing Hexapod Robot with Claws", in *Proc., International Conference on Design Engineering and Science*, 2014, pp. 101-106.
- [7] Jae-Uk S., Donghoon K., ong-Heon J. and Hyun M., "Micro aerial vehicle type wall-climbing robot mechanism", in *Proc., IEEE RO-MAN International Symposium on Robot and Human Interactive Communication*, 2013, pp. 722-725.
- [8] Mahamud N., Muhammad G., Shahriar, H., Sharmin S., and Lisa N. J., "ALW drone: A new design and efficient approach", in *Proc., IEEE 19th International Conference on Computer and Information Technology (ICCIT)*, 2017, pp. 474-479.
- [9] Morita M., Kinjo H., Sato S., Sulyyon T., and Anezaki T., "Autonomous flight drone for infrastructure (transmission line) inspection", in *Proc., IEEE International Conference on Intelligent Informatics and Biomedical Sciences (ICIIBMS)*, 2017, pp. 198-201.
- [10] Lee G., Park J., Kim H., and Seo T. W., "Wall Climbing Robots with Track-wheel Mechanism", in *Proc., IEEE International Conference on Machine Learning and Computing*, 2011, pp.334-337.
- [11] Khirade N., Sanghi R., and Tidke D., "Magnetic Wall Climbing Devices - A Review", in *Proc., International Conference on Advances in Engineering & Technology*, 2014, pp.55-59.
- [12] Kim J. H., Park S. M., Kim J. H., and Lee, J. Y., "Design and Experimental Implementation of Easily Detachable Permanent Magnet Reluctance Wheel for Wall-Climbing Mobile Robot", *Journal of Magnetics* Vol. 15, No. 3, 2010, pp. 128-131.
- [13] Yaguchi H., and Sakuma S., "Vibration Actuator Capable of Movement on Magnetic Substance Based on New Motion Principle", *Journal of Vibroengineering*, Vol. 19, Issue 3, 2017, pp. 1494 - 1508.
- [14] Yaguchi H., and Izumikawa T., "Wireless In-Piping Actuator Capable of High-Speed Locomotion by a New Motion Principle", *IEEE/ASME Transactions on Mechatronics*, Vol. 18, No. 4, 2013, pp. 1367 - 1376.

Copyright © Int. J. of GEOMATE. All rights reserved, including the making of copies unless permission is obtained from the copyright proprietors.
